The Role of Cerium-based Oxides used as Oxygen Storage Materials in DeNOx Catalysis

Xavier Courtois, Nicolas Bion, Patrice Marecot, Daniel Duprez

▶ **To cite this version:**

Xavier Courtois, Nicolas Bion, Patrice Marecot, Daniel Duprez. The Role of Cerium-based Oxides used as Oxygen Storage Materials in DeNOx Catalysis. P. Granger; V.I. Pârvulescu. Past and Present in DeNOx catalysis. From Molecular Modelling to Chemical Engineering, 171 (8), Elsevier, pp.235-259, 2007, Studies in Surface Science and Catalysis, 978-0-444-53058-5. 10.1016/S0167-2991(07)80209-6 . hal-00300635

HAL Id: hal-00300635
https://hal.science/hal-00300635

Submitted on 27 Jan 2021

HAL is a multi-disciplinary open access archive for the deposit and dissemination of scientific research documents, whether they are published or not. The documents may come from teaching and research institutions in France or abroad, or from public or private research centers.

L'archive ouverte pluridisciplinaire **HAL**, est destinée au dépôt et à la diffusion de documents scientifiques de niveau recherche, publiés ou non, émanant des établissements d'enseignement et de recherche français ou étrangers, des laboratoires publics ou privés.

"Past and Present in DeNOx catalysis. From Molecular Modelling to Chemical Engineering" , P. Granger and V. Parvulescu, Eds (Elsevier Sci. Publ.).
Stud. Surf. Sci. Catal., Vol 171. Chapter 8, p. 235-259 (2007).
DOI: 10.1016/S0167-2991(07)80209-6

The Role of Cerium-based Oxides used as Oxygen Storage Materials in DeNOx Catalysis

Xavier COURTOIS, Nicolas BION, Patrice MARECOT and Daniel DUPREZ*

LACCO, Laboratoire de Catalyse en Chimie Organique, CNRS & University of Poitiers, 40 Av. Recteur Pineau 86022 POITIERS Cedex, France.

* Corresponding author: Email: daniel.duprez@univ-poitiers.fr

Abstract

Materials with high "Oxygen Storage Capacity" (OSC) are now widely used in automotive converter catalysts. There are mainly composed of Ce-based oxides (CeZrOx, CeZrPrOx, ...) having both multiple cationic valencies and oxygen vacancies. These properties allow the catalyst to store active O species (O^{2-}, superoxide, ...) in O_2 excess and to release them when the O_2 concentration in gas phase decreases or becomes nil. After having briefly examined the main properties of these OSC materials and the methods employed for their characterization, their impact in automotive catalysis will be reviewed, with a special insight in DeNOx catalysis: (i) in three-way catalysis (TWC) (ii) in automotive catalysis under lean conditions (lean-burn spark ignition engine and Diesel).

1. Introduction

Use of oxygen storage components in three-way catalysis was proposed by Ghandi et al. in 1976 [1] and implemented in the real exhaust catalysts at the beginning of the 80's. Since the pioneer's work of Yao and Yu Yao [2] and of Su et al. [3,4], numerous studies were devoted to a better knowledge of OSC properties of ceria-based compounds [5,6] and, specially, to $Ce_xZr_{1-x}O_2$ mixed oxides [7,8,9,10]. OSC compounds are known to enlarge the "operating window" of TWC, i.e. the λ range within which CO and HC oxidation as well as NOx reduction can occur at the optimal rate (higher than 90% conversion [11]). Although it can be inferred that OSC materials exhibit the highest impact under transient conditions, numerous investigations were carried out at the stationary state. However, kinetic studies carried out at various concentrations may give an idea of what can occur in transient regime.

2. OSC measurements and Oxygen mobility

2.1. OSC measurements

Oxygen storage capacity is generally measured in a pulse chromatographic reactor using CO [12,13,14,15,16] or, to a lesser extent H_2 [17] as reducers. The procedure is depicted in Fig. 1. Pulses of CO (or H_2) are injected over the pre-oxidized sample. According to the nomenclature of Yao and Yu Yao, the CO_2 produced upon the first CO pulse allows to calculate the Oxygen Storage Capacity while the total amount of CO_2 formed upon several CO pulses (typically 10 pulses) gives the "Oxygen Storage Capacity, Complete" (OSCC). In most cases, only OSC is retained for characterizing TW catalysts [18].

Fig. 1 shows the typical behavior of a ceria-based sample. As a rule:

a- The reduction phase (phase 1) is slower than the re-oxidation one (phase 2): the CO_2 formation decreases regularly upon each CO pulse while the re-oxidation is achieved upon the first pulse of O_2. This is a rather general phenomenon in catalysis: oxides (like rare-earth oxides) reduced more slowly than their suboxides may be re-oxidized. It is interesting to note that the reverse phenomenon can be observed with the metals (Pt, Rh, Pd): their oxides are reduced at a much lower temperature than the metal can be re-oxidized [19,20,21] even though the nature of support and the metal particle size may change the redox properties significantly [20,22,23].

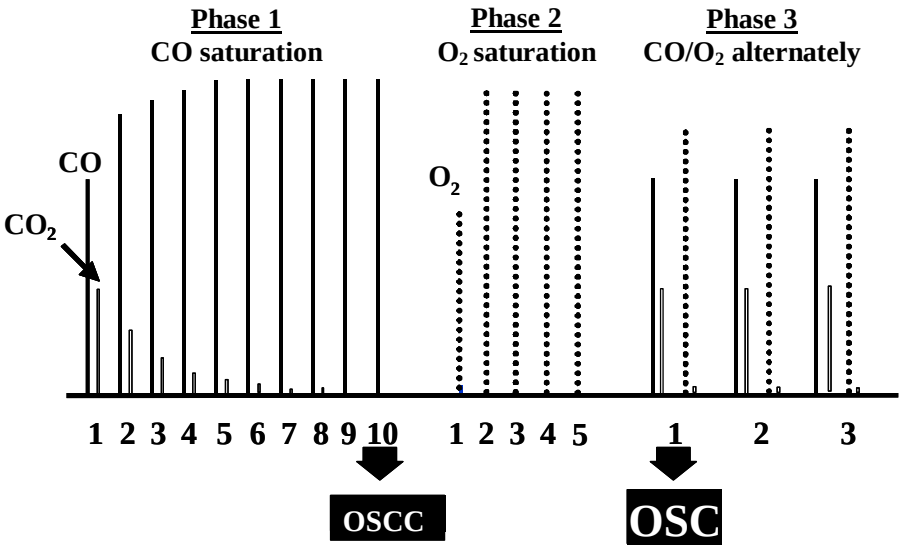

Fig. 1. General procedure for OSC measurements over TWC catalysts. CO and CO_2 are separated over a small Porapak column inserted between the sample and the TC detector. The first CO pulse is injected over pre-oxidized sample. CO can be replaced by H_2.

b- Depending on the temperature, there may be a carbon deficit in the mass balance upon individual pulses, i.e. CO consumption may be higher than CO_2 formation. A certain amount of carbon may be stored in the catalyst and released upon the following CO pulses or upon the first pulses of O_2. In this case, some CO_2 appears in phase 2. A detailed investigation of C and O mass balance during OSC measurements has been made by Holmgren et al [24].

c- In most cases, there is a good agreement between the OSC measured upon the first pulse of CO (phase 1) and the OSC deduced from alternate pulses CO and O_2 (phase 3), which tends to prove that the catalysts show stable redox properties all along the procedure of measurement [25].

Several reaction steps may occur in the course of the oxygen storage process [24,26]:

1- Oxygen adsorption which may be dissociative (Eq. 1) or not (Eq. 2):

$$½O_2 + \square_s \rightarrow O_s \quad (1)$$

$$O_2 + \square_s^{2-} \rightarrow O_2^{2-} \quad (2)$$

where $\square_s$ represents a free vacant site which may be negatively charged as in Eq. 2. Dioxygen species, such as superoxides or peroxides, were evidenced by IR studies [27,28,29].

2- Reaction between CO_g and surface oxygen or dioxygen species to give CO_2 (Eq. 3) or carbonates (Eq. 4)

$$CO_g + O_s \rightarrow CO_{2g} + \square \quad (3)$$

$$CO_g + O_{2s}^{2-} \rightarrow CO_{3s}^{2-} \quad (4)$$

Surface carbonites, carbonates, inorganic carboxylates and sometimes formates (especially at low temperature) were identified by Fourier transform infrared (FTIR) [30,31].

3- Oxygen diffusion from the bulk sites to the surface

$$O_b + \square_s \rightarrow O_s + \square_b \quad (5)$$

4- Side reaction such as CO dissociation (Eq. 6), the Boudouard reaction (Eq. 7) or the water gas shift reaction (Eq. 8, with surface OH species) may also occur:

$$CO_g + 2\square_s \rightarrow C_s + O_s \quad (6)$$

$$2CO_g + \square_s \rightarrow C_s + CO_2 \quad (7)$$

$$CO_g + OH_s \rightarrow CO_2 + ½H_2 + \square_s \quad (8)$$

On ceria or ceria-zirconia, OH_s species are generally associated to the formation of CeOOH groups with a correlative reduction of the surface [32,33].

2.2. OSC of ceria and $Ce_xZr_{1-x}O_2$ oxides

Selected OSC values are reported in Table 1 for ceria and cerium-zirconium mixed oxides. These results confirm that the isomorphous substitution of Ce^{4+} by Zr^{4+} ions clearly improves the catalyst stability. BET area of ceria treated at 900°C is close to 20 $m^2\ g^{-1}$ while it amounts to 35-45 $m^2\ g^{-1}$ for most mixed oxides prepared by coprecipitation or sol-gel methods. Theoretical OSC values may be calculated according to the following assumptions:

- Only Ce^{4+} is reduced into Ce^{3+} in the OSC process. Zr^{4+} virtually cannot be reduced.
- One oxygen atom out of four (among those which are associated with Ce ions) is available in the storage process.

Table 1: OSC values of ceria and $Ce_xZr_{1-x}O_2$ oxides

Catalyst	Tox (°C)	BET area ($m^2\ g^{-1}$)	O Storage		OSC (µmol O)		Ref.
			Red.	°C	g^{-1}	m^{-2}	
CeO_2	900 (6h)	22	CO	400	71	3.2	[9]
$Ce_{0.6}Zr_{0.4}O_2$	900 (6h)	52	CO	400	232	4.5	[9]
CeO_2 NP[a]	900 (4h)	13	CO	400	64	4.9	[10]
$Ce_{0.9}Zr_{0.1}O_2$ NP[a]	900 (4h)	18	CO	400	125	6.9	[10]
$Ce_{0.75}Zr_{0.25}O_2$ NP[a]	900 (4h)	19	CO	400	112	5.9	[10]
$Ce_{0.9}Zr_{0.1}O_2$ SG[b]	900 (4h)	43	CO	400	252	5.9	[10]
$Ce_{0.75}Zr_{0.25}O_2$ SG[b]	900 (4h)	32	CO	400	217	6.8	[10]
Pt/CeO_2	500 (1h)	49	CO	600	250	5.1	[13]
$Pt/Ce_{0.75}Zr_{0.25}O_2$	500 (1h)	72	CO	600	723	10	[13]
Pt/CeO_2	1000 (1h)	2	CO	600	150	75	[13]
$Pt/Ce_{0.75}Zr_{0.25}O_2$	1000 (1h)	14	CO	600	522	37	[13]
CeO_2[c,d]	377 (2h)	5-18	H_2	377	70	6.1	[17]
$Ce_{0.9}Zr_{0.1}O_2$[c,d]	377 (2h)	20-25	H_2	377	280	12.4	[17]
$Ce_{0.65}Zr_{0.35}O_2$[c,d]	377 (2h)	14-18	H_2	377	360	22.5	[17]
CeO_2[c,e]	377 (2h)	5-18	H_2	377	1.2	0.10	[17]
$Ce_{0.9}Zr_{0.1}O_2$[c,e]	377 (2h)	20-25	H_2	377	13	0.58	[17]
$Ce_{0.65}Zr_{0.35}O_2$[c,e]	377 (2h)	14-18	H_2	377	7.5	0.47	[17]

[a] prepared by nitrate precipitation
[b] prepared by a sol-gel technique (Zr propoxide)
[c] prepared by ball milling of oxides
[d] total OSC (value close to OSCC)
[e] dynamic OSC (pulse of H_2)

The theoretical surface density of oxygen ions was evaluated by Madier et al. for different crystallographic planes of CeO_2 and $Ce_xZr_{1-x}O_2$ oxides [14]. For ceria, the theoretical O density would be of 13.7, 9.7 and 15.8 at.O nm^{-2} for (100), (110) and (111) surfaces respectively, which gives a mean surface density of 13.1 at.O nm^{-2} if one assumes an equidistribution of the three crystallographic planes. This figure leads to a theoretical OSC of 5.4 µmol O m^{-2}. The hypothesis of equidistribution may be not valid in all cases which can explains some difference in the reported results. Note that the (111) surface is thermodynamically the most stable.[34,35]

Due to the decrease of the lattice parameter upon Zr substitution, O surface density increases with the Zr content in the materials (see Ref. [36] for a review on the micro and nanostructures of $Ce_xZr_{1-x}O_2$ mixed oxides). The mean oxygen surface density may be approximated by the following equation:

$$S_O\,(\mathrm{at\,O\,nm^{-2}}) = 13.07 + 1.28\,(1-x) \qquad (9)$$

which leads to a theoretical OSC of:

$$OSC_{th}\,(\mu\mathrm{mol\,O\,m^{-2}}) = 5.43\,x + 0.531\,x\,(1-x) \qquad (10)$$

The values of OSC_{th} for the compounds listed in Table 1 are given in Table 2.

Table 2: Theoretical OSC values of $Ce_xZr_{1-x}O_2$ mixed oxides corresponding to the reduction of one surface layer.

x	1	0.9	0.75	0.65	0.60
OSC_{th} (µmol O m^{-2})	5.43	4.93	4.17	3.65	3.39

If one compares the data of Table 1 with the theoretical OSC values given in Table 2 (for one O layer), it appears that:

- the main effect of substituting Ce by Zr is to increase the thermal stability of the materials in significant proportion.
- OSC of $Ce_xZr_{1-x}O_2$ mixed oxides is higher than that of pure ceria. It may also be higher than the theoretical OSC, which proves that several oxygen layers can be involved in the storage process

Comparison of OSC evolutions with temperature for CeO_2 (25 m^2 g^{-1}) and $Ce_{0.63}Zr_{0.37}O_2$ oxide (43 m^2 g^{-1}) was reported by Bedrane et al. [15,37]. Fig. 2 summarizes the specific behavior of these compounds in the oxygen storage process. Up to 300°C, there is virtually no difference between OSC properties of ceria or of $Ce_{0.63}Zr_{0.37}O_2$. By contrast, above 300°C, OSC of the mixed oxide dramatically increases while that of pure ceria remains practically constant.

OSC values at 400 and 500°C for the two samples are compared in Table 3. At these temperatures, the layer number "n" involved in the reduction process is significantly higher for the mixed oxide than for ceria. At 500°C, more than three cerium ion layers (i.e. almost 2 cells) are reduced upon the first pulse of CO.

Table 3: Comparison of OSC of ceria and $Ce_{0.63}Zr_{0.37}O_2$ at 400 and 500°C.

Oxide	OSCth	OSC 400°C (µmol)			OSC 500°C (µmol)		
	m^{-2}	g^{-1}	m^{-2}	n	g^{-1}	m^{-2}	n
CeO_2	5.43	49	1.96	0.36	64	2.56	0.47
$Ce_{0.63}Zr_{0.37}O_2$	3.54	167	3.88	1.10	480	11.2	3.2

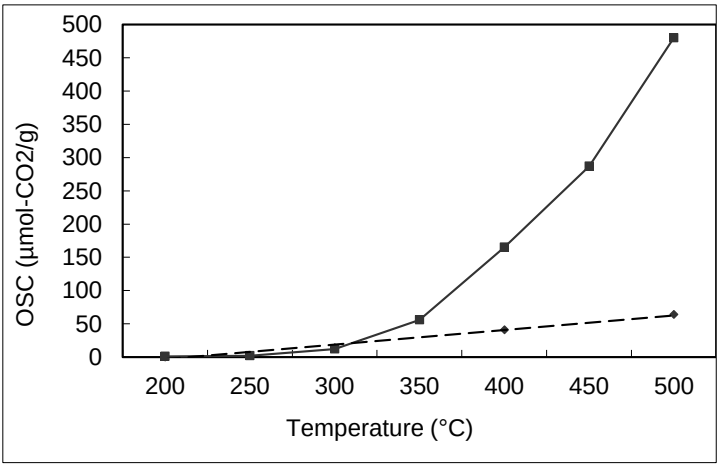

Fig. 2. Evolution of the OSC for CeO_2 (◆) and $Ce_{0,63}Zr_{0,37}O_2$ (■)

2.3. Correlation with oxygen mobility

Oxygen diffusion (Eq. 5) being a crucial step in the global oxygen storage process, OSC measurements have been tentatively correlated to oxygen mobility measured by $^{18}O/^{16}O$ isotopic exchange. The principle has been described in detail elsewhere [14,38,39,40]. It is based on the exchange between gaseous $^{18}O_2$ and ^{16}O species of the support *via* the metal particles (Fig. 3).

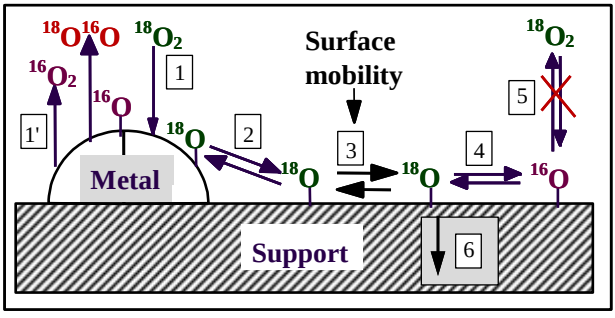

Fig. 3. Measurement of surface diffusion by isotopic exchange.

The reaction is carried out in close-loop reactor connected to a mass spectrometer for $^{18}O_2$, $^{18}O^{16}O$ and $^{16}O_2$ analyses as a function of time [38]. The gases should be in equilibrium with the metallic surface (fast adsorption/desorption steps: 1 and 1'). If the bulk diffusion is slow (step 6) and the direct exchange (step 5) does occur at a negligible rate, coefficients of surface diffusion D_S can be calculated from the simple relationship between the number of exchanged atoms N_e and $\sqrt{t}$ given by the model of circular sources developed by Kramer and Andre [41]:

$$N_e = \frac{2}{\sqrt{\pi}} C_m^{18} I_0 \sqrt{D_s t} \qquad (11)$$

where I_0 is the length of the metal/support interface, i.e. the total perimeter of the metal particles per m^2 of catalyst, and C_m^{18} is the surface concentration (at. m^{-2}) of ^{18}O atoms on the metal. The specific particle perimeter I_0 is a function of the metal loading x_m % and the dispersion D%:

$$I_0 = \beta x_m D^2 \qquad (12)$$

where β is a parameter depending on nature of metal and particle shape. For most metal, β is comprised between 2×10^5 and 10^6 m g^{-1} [40,42] so that the specific perimeter of particles can be greater than 10^8 m g^{-1}. This huge length allows understanding the critical role played by the metal/surface junction in diffusion processes and in catalysis. Eq. 11 is generally applied in the first seconds of exchange: C_m^{18} is then close to the metal surface concentration, all adsorbed O atoms being ^{18}O atoms. Some results obtained by Martin and Duprez [38] with this isotopic exchange technique are reported in Table 4.

Table 4: Relative oxygen surface mobility for some oxides at 400°C (base 10 for alumina). The coefficient of surface diffusion for alumina is 2×10^{-18} m^2 s^{-1}.

Oxides	BET area m^2 g^{-1}	Relative oxygen mobility at 400°C
CeO_2	60	2300
MgO	150	50
ZrO_2	40	28
CeO_2/Al_2O_3	100	18
Al_2O_3	100	10
SiO_2	200	0.1

Ceria shows the highest coefficient of diffusion in the rage of 10^{-15} to 10^{-16} m^2 s^{-1}, which is coherent with the high OSC values obtained with this oxide.

When surface diffusion is the only process of exchange, α_g tends to an equilibrium value α^* at $t \rightarrow \infty$. In most cases, after a rapid step of surface diffusion, it can be observed that α_g continues slowly decreasing. This phenomenon corresponds to a slow step of bulk diffusion (coefficient D_b). A model of bulk diffusion in spherical grains was developed by Kakioka et al which led to the following equation [43]:

$$-\mathrm{Ln}\frac{\alpha_g}{\alpha^*} = \frac{2}{\sqrt{\pi}}\frac{\rho A}{N_g}\sqrt{D_b t} \qquad (13)$$

where A is the BET area of the oxide used as support and ρ its density. Eq. 11 and 13 can be applied for oxides showing a relatively low surface diffusion step. Measurement of D_b could be carried out with alumina and zirconia and was found in the range of 10^{-22} to 10^{-23} m^2 s^{-1} [38]. Interestingly, it was noticed that the bulk O diffusion was an order of magnitude higher in zirconia than in alumina. With ceria, measurement of D_b by Eq. 13 is not possible because of the very fast surface diffusion process, which did not allow discriminating the two regimes of diffusion.

The problem is still more complex with ceria-zirconia samples for which both surface and bulk diffusion occur at a very high rate. A spatio-temporal 3D model was then developed in which all the physical steps (adsorption, desorption, surface and bulk diffusion) involved in the exchange process are taken into account simultaneously [44,45]. A program based on this model was developed and used to determine coefficients of surface and bulk diffusion in CeZrOx-supported metal catalysts. Some results are reported in Table 5 for three Pt/CeZrOx samples [46].

Table 5: Coefficients of diffusion of Pt/CeZrOx catalysts [46].

Catalyst	Pt/CZ-O	Pt/CZ-R	Pt/CZ-D
BET area ($m^2\,g^{-1}$)	104	3	37
Metal particle size (nm)	5.2	59	2
Temperature (°C) of exchange	323	332	334
Surface diffusion D_s ($\times 10^{-20}$ $m^2\,s^{-1}$)	109	1450	1.7
Bulk diffusion D_b ($\times 10^{-23}$ $m^2\,s^{-1}$)	4.5	36	0.34

CZ-O is a conventional mixed oxide prepared by hydrolysis of $ZrO(NO_3)_2$ with an aqueous ammonia solution in the presence of a fine ceria powder. CZ-R was obtained by a reducing treatment in CO at 1200°C while CZ-D was prepared by high energy ball milling of CeO_2 and ZrO_2 powders. This study confirmed that a high temperature of reduction can induce an extremely high mobility in CeZrOx oxides [36].

$^{18}O/^{16}O$ isotopic exchange can detect the presence of binuclear oxygen species (superoxide O_2^-, peroxide O_2^{2-}). When O_2 adsorption leads to the formation of

such species, exchange proceeds via a "multiple exchange" mechanism in which two atoms at once are exchanged:

$$^{18}O_{2g} + \left[^{16}O \bullet\bullet ^{16}O\right]_s \rightarrow ^{16}O_{2g} + \left[^{18}O \bullet\bullet ^{18}O\right]_s \qquad (14)$$

While $^{16}O^{18}O$ is the primary product of exchange in the simple mechanism (exchange atom per atom), $^{16}O_2$ is the primary product when exchange occurs via a multiple mechanism [14,40,47]. This type of mechanism could be linked to the presence of superoxides species which can be detected by FTIR (bands at 1126 cm^{-1}) [48,49]. At the beginning of exchange, the ratio P_{32}/P_{34} is close to 1 on ceria, which means that both mechanisms (simple and multiple) occur with an equal probability. On ceria-zirconia, this ratio is much higher than unity, which implies that the multiple mechanism is predominant [14]. In parallel, exchange of superoxide species can be followed by FTIR. It was shown that $[^{16}O\text{-}^{16}O]^-$ species exchange directly into $[^{18}O\text{-}^{18}O]^-$ ones without intermediary formation of $[^{18}O\text{-}^{16}O]^-$ (Fig. 4). Finally, a clear correlation was observed between OSC and intensity of the band at 1126 cm^{-1}.

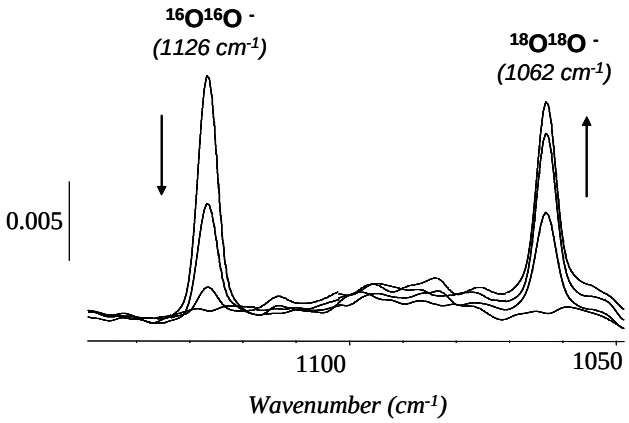

Fig. 4. FTIR spectra of adsorbed superoxide species during exchange of pre-oxidized $Ce_{0.63}Zr_{0.37}O_2$ with $^{18}O_2$. [14]

3. Impact of OSC materials in Three-way catalysts

OSC materials are able to increase the efficiency by enlarging the operating window of TW catalysts [50,51]. NOx reduction in TW catalysts is closely coupled to oxidation reactions since there is a competition between NOx and O_2 reaction on the reducers present in the exhaust gases [52]. We will first examine the effect of these OSC materials on the oxidation efficiency of TW catalysts.

3.1. Impact of OSC on oxidation activity. Steam effects.

Ceria-based OSC compounds may have an impact on oxidation reactions especially when the catalysts are working around the stoichiometry (as this is the case under TW conditions). One of the first systematic studies was reported by Yu Yao [53,54]. Most results were obtained in O_2 excess (0.5%CO+0.5%O_2 or 0.1%HC+1%O_2). Several series of Pt, Pd and Rh/Al_2O_3 of various dispersion, as well as metal foils, were investigated in CO, alkane and alkene oxidation. The effect of metal dispersion in CO and propane oxidation are shown on Fig. 5.

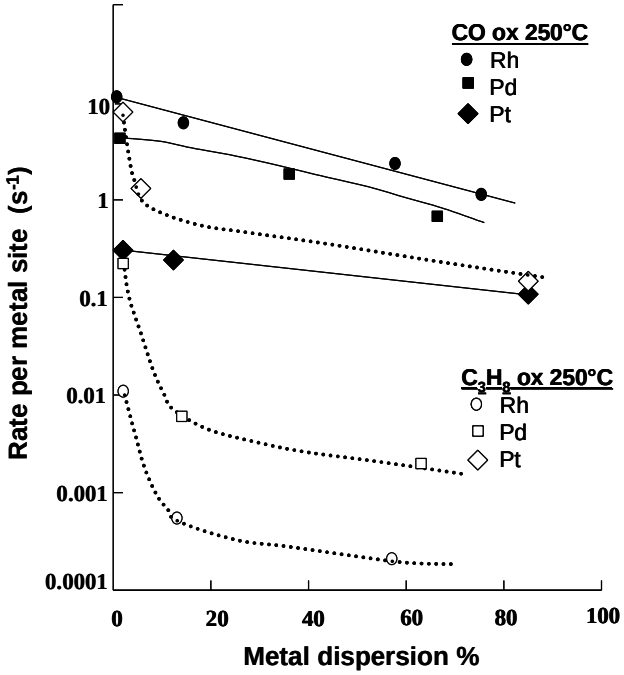

Fig. 5. Effect of metal dispersion on turnover frequencies in CO and propane oxidation (M/Al_2O_3 catalysts). Adapted from the data of Yu Yao [53,54].

In every case, large particles of metal are more active in oxidation than the smallest ones. CO oxidation is moderately structure-sensitive (less than one order of magnitude between metal foil and much dispersed catalysts). By contrast, propane oxidation (and in general oxidation of small alkanes) are strongly structure-sensitive (two orders of magnitude between large and small particles). Rate equations were also expressed as a function of activation energy, E, and kinetic orders with respect to O_2 (m) and to CO or HC (n):

$$r = k_0 \exp(-\frac{E}{RT})\ P_{O2}^{m}\ P_{CO(HC)}^{n} \qquad (15)$$

A summary of the results is given in Table 6. Also reported in the Table are the ratios η between the specific activity of M/CeO_2-Al_2O_3 and M/Al_2O_3 catalysts.

Kinetic orders in CO oxidation on M/Al_2O_3 can be explained by the classical Langmuir-Hinshelwood expression for the rate equation, as a function of the rate constant k, the adsorption constants K and the partial pressures P:

$$r = k\frac{K_O P_O K_{CO} P_{CO}}{(1 + K_O P_O + K_{CO} P_{CO})^2} \qquad (16)$$

Table 6: Kinetic parameters of CO, propane and propene oxidation over M/Al_2O_3 and M/CeO_2-Al_2O_3 catalysts (M = Pt, Pd or Rh).

	CO			C_3H_8			C_3H_6		
	E	m	n	E	m	n	E	m	n
Pt/Al	104-125	+1.0	–0.9	84-105	–1.0	+2.0	67-125	+2.0	–1.0
Pt/Ce-Al	84	+0.5	+0.3	96	–1.0	+2.0	80	+1.5	–0.6
Pd/Al	108-133	+0.9	–0.9	66-96	+0.1	+0.6	63-117	+1.5	–0.5
Pd/Ce-Al	50	0	+1.0	63	+0.1	+0.6	63	+0.7	–0.3
Rh/Al	92-113	+1.0	–0.8	100	0	+0.5	67-92	–0.8	+0.9
Rh/Ce-Al	104	0	+0.2	84	+0.1	+0.4	92	0	+0.5
ηPt	2 (250°C)			0.5 (250°C)			3 (300°C)		
ηPd	1 (250°C).			0.2 (350°C)			0.5 (250°C)		
ηRh	5 (250°C)			3 (400°C)			2 (300°C)		

On alumina, there is a competition between CO and O_2 adsorption on the same metal sites. As CO is much more strongly adsorbed than O_2 on Pt, Pd and Rh, one has: $1 + K_O P_O << K_{CO} P_{CO}$ and Eq. 16 reduces to:

$$r = k\frac{K_O P_O}{K_{CO} P_{CO}}$$, i.e. an order of 1 in O_2 and of 1 in CO. (17)

Eqns 16 and 17 imply that O_2 adsorption is not dissociative, which is coherent with the kinetic data. However O_2 should be dissociated in further steps of the surface reaction. On ceria, new sites for O_2 activation are created at the metal/support interface or in the vicinity of metal particles. As CO and O_2 do not compete with the same sites, the rate equation becomes:

$$r = k\frac{K_O P_O}{1+K_O P_O} \times \frac{K_{CO} P_{CO}}{1+K_{CO} P_{CO}} \qquad (18)$$

with orders between 0 and 1 for CO and O_2, which is again coherent with data of Table 6. Numerous studies on CO oxidation have confirmed these conclusions, most of them differing by the intimate nature of the site for O_2 activation as well as by the chemical state of the metals in the reaction. For Pt/CeO_2-Al_2O_3, Serre et al. [55,56] have described a mixed site Pt-O-Ce, specially created in reducing conditions. The catalyst deactivates after a prolonged exposition in oxidative medium. The presence of specific sites for O_2 adsorption on ceria was elegantly demonstrated by Johansson et al on Pt/CeOx and Pt/SiO_2 catalysts prepared by electron beam lithography [57].On both samples, a kinetic bistability depending on the gas mixing ratio, $\beta = P_{CO} / P_{CO} + P_{O_2}$, can be observed. The bistable region is shifted considerably to much higher β values on Pt/CeOx than on Pt/SiO_2. This could be simulated in kinetic modeling by introducing an oxygen reactant supply via the CeOx support, which maintains a high CO conversion rate even in CO excess.

Similar rate expressions can be derived for propane oxidation. The first step would be the dehydrogenating adsorption of propane on metals giving a CxHy fragment (coverage: θ_C). Contrary to CO, propane is much less strongly adsorbed on the metals than O_2. The order 2 in HC and 1 in O_2 on Pt could be explained by a surface reaction between O_{2ads} and two CxHy species. On Rh and Pd, O_2 shows

a moderate inhibitory effect much less significant than on Pt, kinetic orders being all comprised between 0 and 1.

Clearly, OSC materials improve CO and to a lesser extent HC oxidation in O_2 sub-stoichiometry. OSC materials can also promote reactions of steam with CO (water-gas shift) or HC (steam reforming) [58,59]. Both reactions produce hydrogen (Eq. 19 and 20):

$$CO + H_2O \rightarrow CO_2 + H_2 \quad (19)$$

$$C_nH_m + nH_2O \rightarrow nCO + (n + \frac{m}{2})H_2 \quad (20)$$

The promoter role of ceria in WGS reaction is demonstrated in Fig. 6.

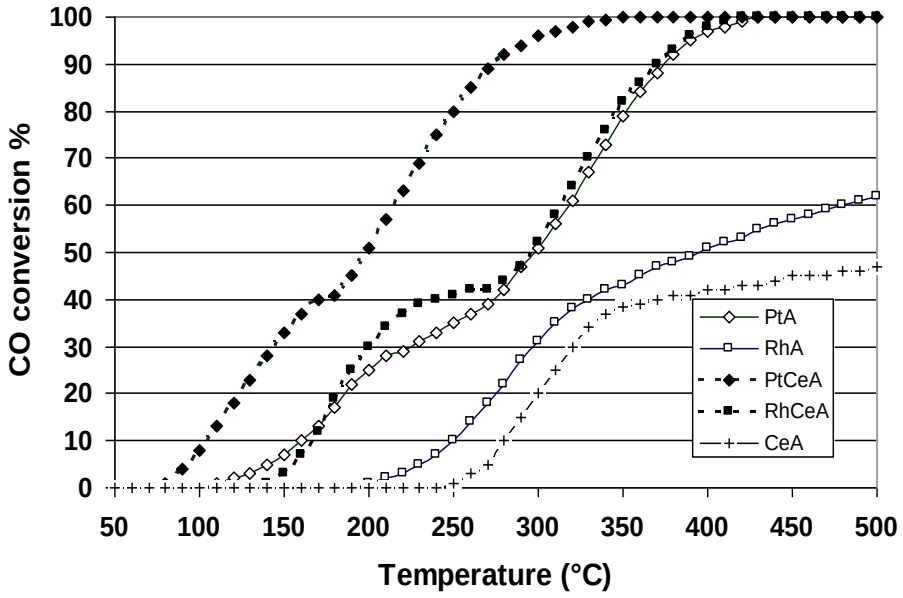

Fig. 6. Temperature-programmed reaction of 0.8%CO in 0.16%O_2+10%H_2O over 1%Pt or 0.2%Rh catalysts supported on alumina (A) or 12%CeO_2-Al_2O_3 (CeA). [58]

Temperature-programmed conversion of CO was carried out in an oxygen-deficient medium. The oxygen content was adjusted to obtain a maximum conversion of 40% by oxidation. The catalysts were 1%Pt and 0.2%Rh deposited over alumina (A) or 12%CeO_2-Al_2O_3 (CeA). The CO conversion is not limited by thermodynamic: it is higher than 99% over the entire range of temperature.

Two regions can be seen on the reaction profiles: the low-temperature domain corresponding to CO oxidation (limited at a 40% conversion) and the high temperature one where the CO having not been oxidized react with water (WGS domain). For every reaction, Pt is the best metal and ceria acts as a promoter. However, an exceptional increase of conversion can be observed in WGS when the metals are deposited on CeA.

Similar experiments were carried out using propane instead of CO as reducer [58]. It was shown that Pt was the best metal for C_3H_8 oxidation while Rh was the most active one in propane steam reforming. Introduction of 12%CeO_2 in the alumina support confirms that CeO_2 rather inhibits C_3H_8 oxidation over Pt while it acts as a promoter on Rh. In both cases, especially with Rh, CeO_2 increases the rate of propane steam reforming.

3.2. Impact of OSC on NO conversion.

The role of OSC materials in NO conversion is more complex. Most metals, specially Rh, are able to decompose NO but this reaction is rapidly inhibited by O species resulting from this decomposition [60]. On Rh, for instance, Rh-O species are replaced by Rh-NO^+ ones in which NO is no longer dissociated [61]. O species may react with adsorbed species of the reducer (CO, HC) to form CO_2. The first role of the OSC materials could be to liberate metal sites by accepting O species.

Indirect effects can also occur, with the Ce^{3+}/Ce^{4+} redox system being able to regulate the metal state (zerovalent or ionic) during richness oscillations.

Reduction of NO by CO

The reaction may lead to N_2 (Eq. 21) or N_2O (Eq. 22).

$$NO + CO \rightarrow ½N_2 + CO_2 \quad (21)$$

$$2NO + CO \rightarrow N_2O + CO_2 \quad (22)$$

For environmental reasons, reaction 21 ($NO \rightarrow N_2$) should be promoted, N_2O having a dramatic greenhouse gas effect. The different steps of reaction 23 have been investigated in detail, mainly by FTIR spectroscopy [61,62,63]. One of the possible intermediate is isocyanate. NCO species could be formed on the metal and migrate on the support, which may explain the large differences observed when Rh is supported on different oxides (alumina, silica, zirconia, ceria-alumina,…). However, the main step should be the dissociative adsorption of NO :

$$NO_g + 2* \rightarrow N* + O* \quad (23)$$

This adsorption reaction has been extensively studied on most noble metals, specially on Rh by NO thermodesorption [64,65,66]. On Rh/ZrO_2 [65], it was shown that N_2 left the surface from two separate features: a sharp β_1 peak at 170°C due to N_2 desorption by reaction (24) and a broad peak (β_2) between 180°C and 430°C corresponding to N_2 recombination (Eq. 25):

$$NO_g + N* \rightarrow N_{2g} + O* \quad (24)$$

$$N* + N* \rightarrow N_{2g} \quad (25)$$

These reactions are very sensitive to particle size of rhodium. On big particles (10 nm), both reaction can occur while, on the smallest ones (3-6 nm), only the recombination feature was observed.

One of the first systematic studies of the NO reduction by CO was reported by Taylor and Kobylinski in 1974 [67]. The reaction was carried out in large excess of CO (0.5%NO+2%CO), which favors the formation of N_2. The light-off temperature T_{50} (50% conversion of NO) allowed ranking the metals (0.5%M/Al_2O_3) by increased activity:

Ru, 205°C > Rh, 296°C > Pd, 431°C > Pt, 471°C

Except Ru (not usable in TWC because of the volatility of its oxide [68]), the most active metal is the rhodium. This has been largely confirmed by further studies so that Rh may be considered as a key-component of TWC for NO reduction [69,70]. As far as Pd is concerned, it seems that the active site is composed of Pd^{n+}-Pd^0 pairs, which may explain the higher activity of Pd in NO+CO+O_2 mixture ($T_{50} \approx$ 200°C) [71]. A detailed kinetic study by Pande and Bell on Rh catalysts has evidenced a significant support effect [72]. The kinetic data were represented by a conventional power law expression:

$$R_{NO} = k_{NO}\, P_{NO}^{\alpha}\, P_{CO}^{\beta} \qquad (26)$$

where R_{NO} is the reaction rate per second and per metal site, P, the pressure in atm, and k_{NO} the kinetic constant in atm $^{-(\alpha+\beta)}$ s^{-1}.

The main results are reported in Table 7.

Table 7: Kinetics of the CO+NO reaction at 210°C over Rh catalysts. Gas composition is 1.3%NO+3.9%CO [72]

Catalyst	BET area $m^2\ g^{-1}$	Dispersion %	Order /NO	Order /CO	Ea kJ mol^{-1}	k_{NO} 10^{-3}
4.6% Rh/SiO_2	250	55	–0.2	+0.1	140	4.30
4.2% Rh/Al_2O_3	175	64	–0.4	~0	101	0.82
4.6% Rh/MgO	100	46	–0.2	+0.1	108	2.92
4.3% Rh/TiO_2	50	26	+0.1	–0.2	82	7.75
4.2% Rh/La_2O_3	14	10	–0.2	~0	126	4.75

The different catalysts may be ranked according to their relative activity:

TiO_2, 9.5 > La_2O_3, 5.8 > SiO_2, 5.2 > MgO, 3.6 > Al_2O_3, 1

Between 100 and 200°C, the selectivity to N_2O is very high (70-85%) and decreases with the temperature in accordance with most of the studies on the reduction of NO by CO.

The kinetics of this reaction (1.5%NO+3%CO, 200°C) on a 1%Rh/SiO_2 catalyst promoted by Mo, Ce and Nb (1 to 10 wt-%) was studied by Hecker et al. [73]. A significant particle size effect was observed: the biggest particles of Rh are the most active per Rh site (Fig. 7). On silica, the promoter effects are mainly due to particle size effects: certain promoters, especially ceria being able to stabilize Rh particles. The presence of Mo tends to slow down the reaction so that Mo appears as an inhibitor of the reaction. Kinetic parameters obtained by Hecker et al. are close to those reported by Pande and Bell: orders slightly negative in NO (−0.2 to −0.5, exceptionally −1.2 for Mo) and orders nil or slightly positive with respect to CO (0 to +0.4); activation energies between 117 and 139 kJ mol^{-1}.

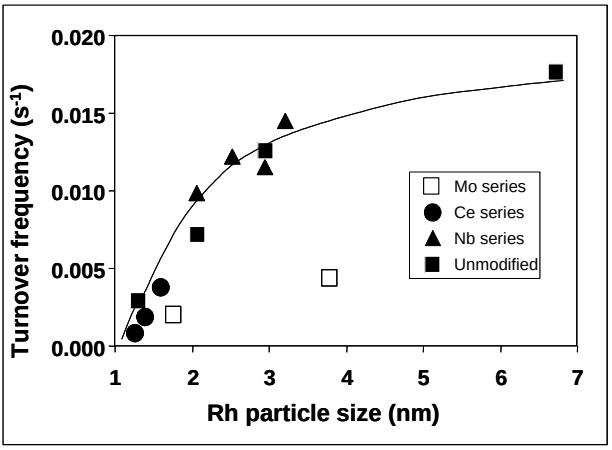

Fig. 7. Effect of the dispersion of Rh on the NO reduction by CO at 200°C over promoted Rh/SiO_2 catalysts (1.5%NO+3%CO) [73].

The reduction of NO by CO was investigated in detail by Oh et al. in closer conditions than those encountered in automotive converters: weaker NO and CO concentrations, close to the stoichiometry, more realistic metal content (< 1%) [74,75]. The main conclusions of Oh's works are:

- the high sensitivity of the reaction to particle size of Rh is confirmed: at 230°C, in a mixture of 0.5%NO + 1%CO, the turnover frequency increases from 0.017 s^{-1} for a highly dispersed catalyst to 0.74 s^{-1} for a catalyst dispersed at 1.7%, the activity per metal site on unsupported Rh catalysts being still much higher.
- ceria remarkably increases the activity of Rh/Al_2O_3: 2 to 9 wt-% CeO_2 added to a 0.014%Rh/Al_2O_3 catalyst increases its activity by a factor 5 by 250°C. However, ceria decreases the activation energy (120 kJ mol^{-1} on Rh/Al_2O_3: instead of 80 on Rh/CeO_2-Al_2O_3) so that the two catalysts have nearly the same activity around 300-310°C.
- the reaction CO+NO may be seen as an oxidation of CO by NO which competes with the oxidation of CO by O_2. On Rh, CO oxidation by dioxygen is almost two orders of magnitude faster than CO oxidation by NO. Nevertheless, if the three reactants are present together, the rate of CO oxidation by O_2 dramatically decreases while that of CO by NO increases. As a consequence, both reactions occur practically at the same rate [76].

Most of the kinetic observations can be interpreted as follows:

- the key-step is the NO decomposition (Eq. 23): the global reaction rate depends for a great part of the rate of this step.
- at low temperature, N_2 is mainly formed by the reaction of NO_g with adsorbed N* species (Eq. 24) or by the same reaction with adsorbed NO (Eq. 27):

$$NO* + N* \rightarrow N_2 + O* + * \qquad (27)$$

while N_2O is formed by a similar reaction (Eq. 28):

$$NO* + N* \rightarrow N_2O* + * \quad (28)$$

At high temperature, NO is almost totally dissociated: N_2O cannot then be formed and N_2 stems essentially from recombination of adsorbed N* species (Eq. 25). The selectivity to N_2 increases with the temperature and virtually reaches 100% around 300°C (Fig. 8).

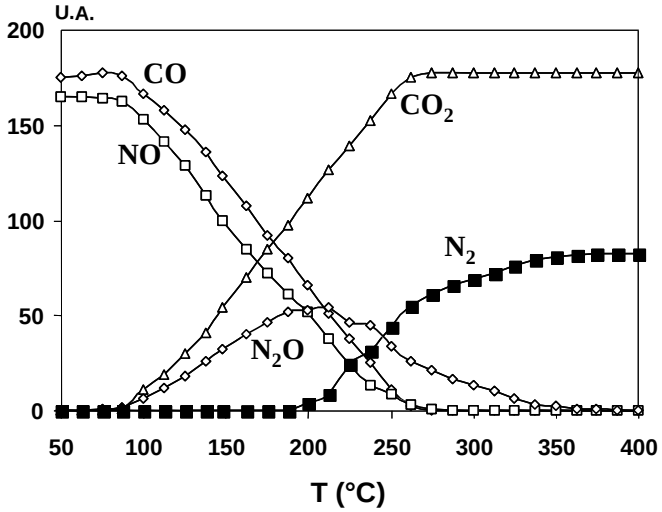

Fig. 8. Temperature-programmed reaction of CO (1%) + NO (1%) over a pre-oxidized 0.2%Rh/CeO_2-Al_2O_3 catalyst [77]

The chemical state of the metal can play a decisive role on the reaction mechanism. In TWC, Rh is thought to remain in the zero valent state, which favors NO dissociation [78,79]. However, the role of the OSC materials is complex and it is not inert with respect to NO activation. Ranga Rao et al. [80] showed that, when bulk oxygen vacancies are formed in a reduced $Ce_{0.6}Zr_{0.4}O_2$ solid solution, NO was efficiently decomposed on the support to give N_2O and N_2. Further studies by the same group using different $Ce_xZr_{1-x}O_2$ composition and different metals confirmed

this prominent property of supports containing reduced ceria [81,82]. Selected results of these studies are reported in Table 8.

A significant increase of activity can be observed on Rh catalysts supported on reducible oxides. Activity exaltation is severely annihilated when the catalysts are treated in the reaction mixture. Nevertheless, the presence of chlorine largely upset the results: Cl probably slows down the reduction of the support, particularly in the CO+NO mixture.

By surface science techniques, Mullins and Overbury showed that the presence of reduced ceria might create new active sites for NO dissociation [83]. The degree of decomposition is increased and the onset temperature for decomposition is reduced when Rh is supported on reduced ceria (Rh/CeO_x) compared to Rh on oxidized ceria (Rh/CeO_2) NO dissociation being self-inhibiting.

Table 8: Effect of the reducing pretreatment of 0.5 %Rh catalysts on the NO+CO reaction rate (1% NO+1%CO) [81,82].

Support	Rh precursor	Reaction rate at 200°C after pretreatment in H_2, for 2h at 200°C (mole NO g^{-1} $s^{-1}\times10^9$)	Reaction rate at 200°C after pretreatment in CO+NO from 200 to 500°C (mole NO g^{-1} $s^{-1}\times10^9$)
Al_20_3	Chloride	70	32
$Ce_{0.4}Zr_{0.6}O_2$	Chloride	331	90
$Ce_{0.6}Zr_{0.4}O_2$	Chloride	336	46
CeO_2	Chloride	1120	83
$Ce_{0.6}Zr_{0.4}O_2$	Nitrate	1630[a]	1590[a]

[a]Reaction rate at 160°C

The promotion by reduced ceria could be due to a spill-over phenomenon of O species from metal to support. In fact, this is not sufficient to explain all the results of Mullins and Overbury: an exposure of the Rh/CeOx surface to water leads to a

re-oxidation accompanied by a hydroxylation of the support while the metal surface is left unchanged. In fact, it seems that preferential orientation of Rh surface on reduced ceria may also explain the specific role of CeOx surface. This is consistent with the fact that NO dissociation occurs at lower temperatures on Rh (110) and on Rh (100) than on Rh (111) [84,85].

However, reduced ceria is able, alone, to dissociate NO. Martinez-Arias et al. [86] have first investigated by EPR and FTIR spectroscopies NO reaction on ceria pre-outgassed at different temperatures and showed the role of superoxides differentially coordinated in the formation of hyponitrites species further decomposed into N_2O. Later Haneda et al. [87] have demonstrated that reduced ceria and reduced praseodymium oxide dissociate NO even though the presence of a noble metal (Pt) significantly increases the formation of N_2 or N_2O. The main results of this study are summarized in Table 9.

Lanthanum and samarium shows virtually no NO dissociation activity even in the presence of Pt. These supports are not reducible and have no OSC property. The intrinsic NO dissociation activity of platinum is very weak, probably in reason of the low metal dispersion. The behavior of terbium oxide is more surprising: although it is reducible in H_2, it is unable dissociating NO except in the presence of Pt.

The specific role of OSC materials in NO activation and NO dissociation has largely been confirmed by many authors over Pt-Rh [88,89] and Pd catalysts [90,91] or even over bare OSC oxides [92]. By EPR, Lecomte et al. [88] evidence the presence of O_2^- superoxide species over a Pt-Rh/Al_2O_3 catalyst modified by ceria. The formation of these species could be closely related to the performance of the Pt-Rh/CeO_2-Al_2O_3 catalyst in CO+NO reaction.

Table 9: NO dissociation over reduced rare-earth oxides and over 1%Pt catalysts deposited on these oxides. Prior to NO dissociation (970 ppm NO), the samples are reduced for 1h in H_2 at 500°C [87].

	BET area $m^2\,g^{-1}$	H_2 TPR (25-500°C)	N_2 (N_2O) formed mmol g^{-1}	
RE oxide		µmol H_2 g^{-1}	at 200°C	at 400°C
La_2O_3	7.5	2.5		0.0 (0.0)
CeO_2	55	75		14.7 (2.6)
Pr_6O_{11}	9.5	773		19.6 (4.6)
Sm_2O_3	8.0	1.5		0.0 (0.0)
Tb_4O_7	22	1008		0.0 (0.0)
Pt/RE oxides				
Pt/La_2O_3		17	0.0 (0.0)	1.8 (0.2)
Pt/CeO_2		271	50.0 (1.1)	52.3 (0.0)
Pt/Pr_6O_{11}		1823	225 (226)	431 (10.5)
Pt/Sm_2O_3		41	0.0 (0.0)	5.5 (0.2)
Pt/Tb_4O_7		1356	27.2 (8.1)	248 (0.0)

When the ceria-containing catalyst is pre-reduced before reaction, a typical temperature-programmed reaction profile can be observed (Fig. 9). While prereducing the catalyst has virtually no effect on Pt-Rh/Al_2O_3, a significant activity peak can be observed at low temperature on the ceria-based catalyst. This peak disappears upon calcination and a profile like that of Fig. 9 can then be recorded. It is not systematically recorded in bench tests with complex synthetic mixtures [93].

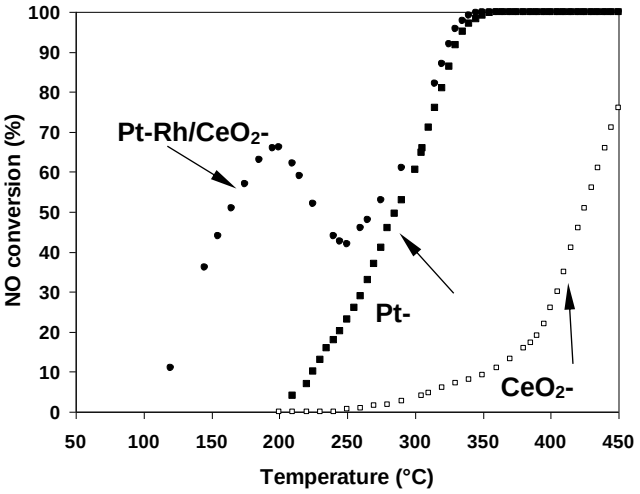

Fig. 9 Effect of ceria on the NO reduction by CO
(Gas composition: 0.5%NO+0.5%CO, 25000 h^{-1}). After Ref. 88.

The behavior of CeO_2-Al_2O_3 support is rather general and can be observed with other ceria-containing catalysts such as Rh/CeO_2-ZrO_2 catalysts [81,82] or Pd/ CeO_2-ZrO_2 [94]. It has also been shown that pre-reduced ceria-zirconia supports present a noticeable activity in NO+CO in the absence of metal. This activity totally disappears when the support is calcined [89].

Reduction of NO by H_2 and hydrocarbons

Compared to CO, these reactions were much less studied over TW catalysts. Kobylinski and Taylor [67] have compared the NO reduction by CO and by H_2. Their main results are summarized in Tables 10 (light-off activity) and 11 (selectivity).

Table 10: Temperatures (T°C) for 50% NO conversion as a function of the reducing agent. Catalysts: 0.5% metal on alumina. Space velocity: 24000h^{-1}.

Catalyst	NO + H_2	NO + CO	NO + CO + H_2
Pt	121	471	398
Pd	106	431	330
Rh	163	296	275
Ru	237	205	210

Table 11: Product selectivity (% NO converted in N_2 and NH_3) and reaction selectivity (%NO converted by NO+CO and NO+H_2). Gas composition 1.5 % NO + 4.5% CO + 4.5 % H_2.

Catalyst	T (°C)	NO conv. %	Selectivity				%N_2 from NO+CO
			NO→N_2	NO→NH_3	NO+CO	NO+H_2	
Pt	515	94	23	77	8	92	40
Pd	515	94	26	74	9	91	38
Rh	482	100	67	33	20	80	29
Ru	432	100	92	8	29	71	31

Pt and Pd are by far the most active metals in NO reduction by H_2 while Rh and Ru present the highest activity in NO reduction by CO. However, when the two reducers are injected together (last column), CO tends to impose its behavior in NO reduction. This is due to a strong adsorption of CO, which inhibits the reduction by H_2.

Although CO seemed to inhibit the reduction by H_2, this reducer still maintains a very significant activity. The CO inhibition is largely compensated by the high temperature of working. Interestingly, Table 11 confirms the good selectivity of Rh (and Ru) to N_2 while Pt and Pd lead to a significant formation of ammonia. Maunula et al. [95] have confirmed the superiority of Pt over Rh in the reduction

of NO by H_2. They also found that N_2O would be an intermediate in the formation of N_2.

Relatively few studies were devoted to the reduction of NO by HC in TW conditions. Platinum seems to be a good reducer of NO by light alkanes, specially the methane [96]:

$$CH_4 + 4NO \rightarrow 2N_2 + CO_2 + 2\ H_2O \qquad (29)$$

However, some contradictory results were obtained in several studies. For instance, in the CH_4-NO reaction, some authors have reported that N_2O was the primary product [96] while others found that ammonia was first produced [97]. The presence of water can play a decisive role since H_2O allows generating H_2 by WGS or steam reforming [59]. Olefins generally show a higher activity than alkanes: propene for instance has been found more reactive than propane. Some exceptions should be quoted, ethylene having been found less reactive than CH_4 in NO reduction at stoichiometry [98].

The role of ceria is practically not evoked in these previous studies. More recently, Pérez-Hernández et al. have compared the catalytic behavior of Pt/ZrO_2, Pt/CeO_2 and Pt/CeO_2-ZrO_2 in NO reduction by CH_4 or CO [99]. All the catalysts were found more active and more selective to N_2 in NO reduction by CH_4. However the cerium content plays a decisive role in decreasing the differences of NO light-off activity between CH_4 + NO and CO + NO. Rather different results were obtained by Bera et al. [100] who found Pt/CeO_2 more active in CO+NO (100% conversion achieved at 270°C) than in NO+CH_4 (100% conversion at 350°C). However, the superiority of the ceria support with respect to alumina in NO reduction was demonstrated both for Pt and Pd catalysts. As said before, ceria may also modify the catalyst behavior by increasing the H_2 content in rich conditions, which may induce a higher capacity of the catalyst to reduce NO.

A close parallelism could be established between the OSC of aged catalysts and their light-off activity in CO, HC and NOx conversion [101]. Different evolutions of both the OSC and the catalytic activity were observed depending on the method of ageing (laboratory ageing or engine bench ageing) and on the type of catalyst (PtRh/ CeO_2-Al_2O_3 or PdRh/ CeO_2-Al_2O_3). In every case, the conversion of NOx is the most sensitive to catalyst ageing. This has been confirmed by Muraki and Zhang who compared CO, HC and NO conversions over aged Rh catalysts supported on ceria and ceria-zirconia [70]: the conversions were significantly higher over ceria-zirconia supported Rh catalysts, much more stable than those supported on pure ceria. Ageing the catalyst, especially in rich/lean oscillation, may also leads to heterogeneity in the Ce local concentration. Finally, possible migration of Ce^{4+} ions was observed by Fan et al. in $Pt/Ce_{0.67}Zr_{0.33}O_2$ catalyst in rich/lean oscillations. Cerium ions may then decorate Pt particles and deeply modified their behavior in NO reduction [102].

4. Impact of OSC materials in lean-burn and Diesel catalysis

The impact of oxygen storage in DeNOx catalysis in O_2 excess is more complex and strongly depends on the process used for NOx reduction. The impact of OSC materials will be examined on two processes: the selective reduction by HC (HC-SCR) and the NOx-trap process.

4.1. Impact of OSC materials in HC-SCR

In the 90's, most investigations were devoted to passive DeNOx, i.e. NOx reduction by the HC present in the exhaust gas. Even in lean conditions, there remains Ce^{3+} cations and oxygen vacancies which may participate in NO or HC

activation. In 2000, Djega-Mariadassou et al. [78] proposed the following model for NO adsorption in Rh/CeO_2 where Rh is partially oxidized while there remain reduced sites of ceria on the support (Fig. 10)

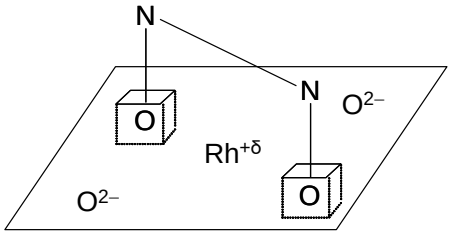

Fig. 10. Model of adsorption site for NO in the presence of O_2 (adapted from Ref. 78). The cubes represent oxygen vacancies. $Rh^{+\delta}$ would be the site for HC (or CO) activation.

However, there are also evidences that Ce^{3+} cations could participate in NO activation and dissociation [86,103,104]. The model of Fig. 10 was later modified to take into account this possibility [105]. It seems that the behavior of Pd/CeO_2-ZrO_2 can be explained by similar models of NO and HC activation [106]: NO would be adsorbed on reduced sites of ceria-zirconia while the hydrocarbon (propylene in this study) would be partially oxidized into $C_xH_yO_z$ intermediates over PdOx sites. For the reduction of NO in oxygen excess, it seems however that conventional catalysts, even doped with OSC materials, cannot adsorb the HC's to reduce the NOx efficiently. Engineers of Toyota have proposed a system composed of a dual bed in which the conventional Pt catalyst is mixed with different zeolites [107]. A relatively close contact between Pt and the zeolite which stores the HC's is required but the advantage of this technique is that the zeolite as well as the presence of an OSC materials prevent the poisoning of Pt by heavy HC's. Some experiments were carried out with Pt in the zeolite but the most interesting system would the multi-component catalyst schematized in Fig. 11.

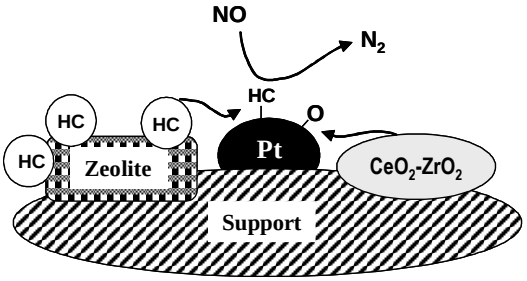

Fig. 11. Cooperative effect of an OSC component and a zeolite in SCR-HC of NO in O_2 excess.

The idea to insert an OSC component such as Ce ions in zeolite has received much attention. Cordoba et al [108] have shown that H-ZSM5 promoted both by Ce and Pd has excellent properties in lean-DeNOx by dodecane (Fig. 12). As in the previous example (Fig. 11) the zeolite should help storing and probably transforming the dodecane molecule into highly reducing species. Thanks to their redox properties, Ce ions could adsorb NO and maintain Pd in the better chemical state to reduce NO.

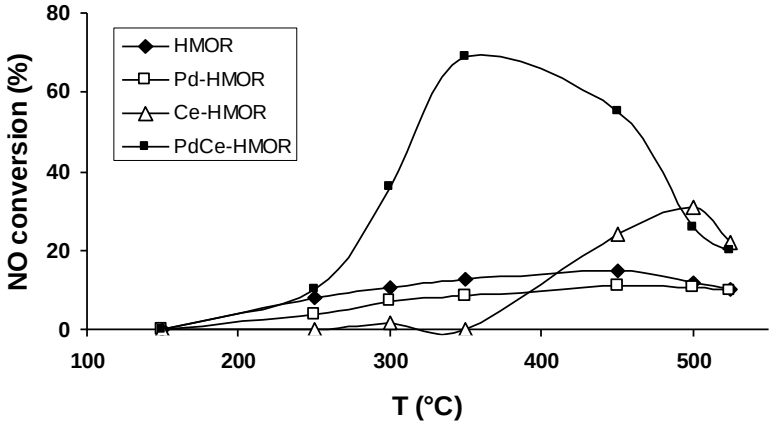

Fig. 12. Cooperative effect of Pd and Ce in lean-DeNOx by dodecane (900 ppm NO + 100 ppm NO_2 + 30 ppm N_2O + 400 ppm $C_{12}H_{26}$ + 6%O_2 [108].

Very few studies were devoted to NO reduction by H_2 in lean conditions because of the high reactivity of H_2 with O_2. Costa et al [109,110] discovered a new low loaded Pt catalyst able to perform H_2-DeNOx with a good selectivity. It consists of 0.1 %Pt supported on $La_{0.5}Ce_{0.5}MnO_3$. This catalyst was found very active (74% NO conversion at 140°C in a mixture 0.25% NO, 1% H_2, 5%O_2, 5%H_2O/He, GHSV: 80,000h^{-1}) and more selective to N_2 (87% at 140°C) than a conventional 0.1%Pt/alumina catalyst [109]. By transient isotopic exchange reaction, Costa and Efstathiou showed that the interface metal/support played a significant role in NO reduction. Two kinds of active NOx species were evidenced: M-NO_2^+ located on the $La_{0.5}Ce_{0.5}MnO_3$ support and M-O-(NO)-O-M at the interface metal/support, while on a non-selective Pt catalyst, virtually all the active species are on Pt (Pt-$NO^{\delta+}$ or Pt-nitrate) [110].

4.2. Impact of OSC materials on NOx-trap systems

One of the most promising processes is the active DeNOx based on NOx-trap materials. It has been developed for lean-burn gasoline engines. Cerium compounds are thought to intervene in different steps of the whole process: (i) NO oxidation, (ii) NOx storage; (iii) Nitrate desorption and NOx reduction. Most probably, the main role of OSC materials is to accelerate HC partial oxidation during rich-spikes (giving CO and H_2 as NOx reducers). However, this beneficial effect of OSC compounds competes with a detrimental reaction, i.e. the reduction of the OSC materials itself that may delay HC decomposition and thus NOx reduction [111]. Nakatsuji et al. [112], in cooperation with researchers of Isuzu, have studied the effect of OSC materials on simplified catalysts inasmuch as Rh was directly deposited on oxides known for their OSC properties (Ce, Ce-Zr, Ce-Pr, Ce-Nd-Pr, Ce-Gd-Zr oxides). These catalysts were submitted to periodic lean

(55s)/rich (5s) excursions as in the conventional NOx-trap system. Compared to non-OSC supports, ceria allows maintaining a high DeNOx activity even in large O_2 excess during the lean period (Fig. 13).

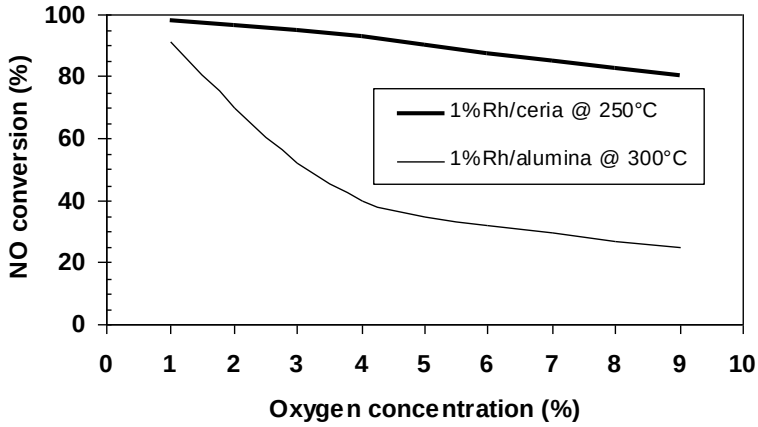

Fig. 13. Effect of O_2 concentration over Rh-loaded catalysts at the temperature of their max. activity (lean/rich spans: 55/5s; 50,000 h^{-1}).

Even in absence of the classical Ba component, OSC materials may play a role in the NOx reduction using severely lean/rich conditions.

Most of other studies implying OSC materials were devoted to the chemical interaction between the NOx-trap materials (Ba) and the OSC oxides. The order of introduction of the different functions (metal=Pd, OSC and NOx-trap) was studied by Kolli et al. [113]. Although the aim of this work was to study the catalysts in TWC conditions, some interesting results were obtained which may be generalized to other conditions. It was shown that the best catalysts consisted of Pd-Ba or Ba-Pd deposited over OSC-Al_2O_3 support, i.e. the OSC materials should be impregnated first. Although their catalyst was not optimized, Liotta et al. [114] have investigated a Pt-OSC/Ba-Al_2O_3 catalyst in NOx-trap conditions. Interestingly, they showed that Ba ions migrated through the OSC layer (CeZrOx).

This property could allow a better control of the Ba dispersion as well as an increased resistance to SO_2 poisoning. However the presence of Ba is not essential for the NOx-trap when OSC material is used as support. Eberhardt et al. [115] and Philipp et al. [116] have compared the NOx trap behavior of Ba/Al_2O_3 and Ba/CeO_2 materials. Ba/CeO_2 show higher NOx storage efficiency than Ba/Al_2O_3 within the temperature range of 200-400°C. No solid/solid reaction between Ba and ceria was observed below 780°C while Ba reacted at lower temperature with Al_2O_3 to form inactive Ba aluminate. In these previous studies, however, no noble metal was impregnated on the support, which may bias the results in real catalysts. Corbos et al. have compared the NOx storage capacities of Pt/CeZrOx with a classical $Pt/Ba/Al_2O_3$ and with Pt/Ba/CeZrOx. The values given in Table 12 show a better capacity for Pt/CeZrOx at certain temperatures [117].

Table 12: NOx storage capacities ($\mu mol.g^{-1}$) calculated for the first 100 seconds. The catalysts were stabilized at 700°C under O_2, H_2O, N_2; Storage mixture : 350ppm NO, 10%O_2, 10%H_2O, 10%CO_2 and N_2. (Ref. 117)

	NOx storage capacities ($\mu mol.g^{-1}$)		
Storage temperature (°C)	200	300	400
Pt/Ba/Al (129 $m^2.g^{-1}$)	13.1	13.7	18.3
Pt/CeZr (61 $m^2.g^{-1}$)	17.1	14.6	15.0
Pt/Ba/CeZr (47 $m^2.g^{-1}$)	9.4	11.8	23.3

Similar results were obtained by Lin et al. [118] who investigated the effect of La and Ce on NOx storage properties of $Pt/Ba\text{-}Al_2O_3$. Substituting La for Ce increased the NOx storage capacity from 341 µmol g^{-1} in $Pt_{2.5}La_{30.5}Ba_{33.4}Al_{100}$ to 1020 µmol g^{-1} for the $Pt_{2.5}Ce_{30.5}Ba_{33.4}Al_{100}$ catalyst.

Finally, unconventional OSC supports have also been investigated. Machida et al, for instance, studied a Pd/MnOx-CeO_2 as NOx-storage materials [119]. This catalyst was tested in lean/rich conditions using H_2 as reducer with, however, an unusual period (9 min. lean/3 min. rich). The catalyst showed both excellent activity and selectivity (almost 100% to N_2).

References

[1] H. S. Ghandi, A. G. Piken, M. Shelef, R. G. Deloch, SAE Paper 760201 (1976).
[2] H. C. Yao, Y. F. Yu Yao, J. Catal. 86 (1984) 254.
[3] E. C. Su, C. N. Montreuil, W. G. Rothschild, Appl. Catal. 17 (1985) 75.
[4] E. C. Su, W. G. Rothschild, J. Catal. 99 (1986) 506.
[5] B. Engler, E. Koberstein, P. Schubert, Appl. Catal. 48 (1989) 71.
[6] T. Miki, T. Ogawa, M. Haneda, N. Kakauta, A. Ueno, S. Tateishi, S. Matsuuta, M. Sato, J. Phys. Chem. 94 (1990) 6464.
[7] M. Ozawa, M. Kimura, A. Isogai, J. Alloys Comp. 193 (1993) 73.
[8] P. Fornasiero, R. Di Monte, G. Ranga Rao, J. Kašpar, S. Meriani, A. Trovarelli, M. Graziani, J. Catal. 151 (1995) 168.
[9] J. P. Cuif, G. Blanchard, O. Touret, A. Seigneurin, M. Marczi, E. Quéméré, SAE Paper Nr 970463 (1997).
[10] S. Rossignol, F. Gérard, D. Duprez, J. Mater. Chem. 9 (1999) 1615.
[11] E.S.J. Lox and B.H. Engler in “Environmental Catalysis”. G. Ertl. Et al. eds. Wiley-VCH 1999, p. 1
[12] S. Kacimi, J. Barbier Jr, R. Taha, D. Duprez, Catal. Lett. 22 (1993) 343.
[13] C. E. Hori, H. Permana, K. Y. Simon Ng, A. Brenner, K. More, K. M. Rahmoeller, D. Belton, Appl. Catal. B, 16 (1998) 105.
[14] Y. Madier, C. Descorme, A. M. LeGovic, D. Duprez, J. Phys. Chem. B 103 (1999) 10999.
[15] S. Bedrane, C. Descorme, D. Duprez, Catal. Today, 73 (2002) 233.
[16] E. Rohart, O. Larcher, C. Hédouin, M. Allain, P. Macaudière, S. Deutsch SAE Paper 04-01-1274 (2004).
[17] A. Trovarelli, F. Zamar, J. Llorca, C. De Leitenburg, G. Dolcetti, J. T. Kiss, J. Catal. 169 (1997) 490.
[18] D. Duprez, C. Descorme in "*Catalysis by Ceria and Related Materials*" (A. Trovarelli, Ed.) , Chapter 7, p. 243-280, Imperial College Press (2002).
[19] J. Barbier, D. Bahloul, P. Marécot, J. Catal. 137 (1992) 377.
[20] D. Martin, D. Duprez, Appl. Catal. A, 131 (1995) 297.
[21] A. M. Pisanu, C. E. Gigola, Appl. Catal. B 11 (1996) L37.
[22] A. Douidah, P. Marécot, S. Szabo, J. Barbier, Appl. Catal. A 225 (2002) 21.

[23] H. Yoshida, Y. Yazawa, T. Hattori, Catal. Today 87 (2003) 19.
[24] A. Holmgren, B. Andersson, D. Duprez, Appl. Catal. 22 (1999) 215.
[25] S. Rossignol, C. Descorme, C. Kappenstein, D. Duprez, J. Mater. Chem. 11 (2001) 2587.
[26] S. Bedrane, C. Descorme, D. Duprez, Catal. Today, 75 (2002) 401.
[27] J. Soria, A. Martinez-Arias, J. Conesa, J. Chem. Soc. Faraday Trans. 91 (1995) 1669.
[28] C. Li, K. Domen, T. Maruya, T. Onishi, J. Am. Chem. Soc. 111 (1989) 7683.
[29] C. Descorme, Y. Madier, D. Duprez, J. Catal. 196 (2000) 167.
[30] C. Li, Y. Sakata, T. Arai, K. Domen, K. Maruya, T. Onishi, J. Chem. Soc. Faraday Trans. 1 85 (1989) 929; C. Li, Y. Sakata, T. Arai, K. Domen, K. Maruya, T. Onishi, J. Chem. Soc. Faraday Trans. 1 85 (1989) 1451.
[31] C. Binet, A. Badri, M. Boutonnet-Kizling, J. C. Lavalley, J. Chem. Soc. Faraday Trans. 90 (1994) 1023.
[32] M. Daturi, E. Finnochio, C. Binet, J. C. Lavalley, F. Fally, V. Perrichon, J. Phys. Chem. B 103 (1999) 4884.
[33] A. Norman, V. Perrichon, Phys. Chem. Chem. Phys. 5 (2003) 3557.
[34] T. X. T. Sayle, S. C. Parker, C. R. A. Catlow, Surf. Sci. 316 (1994) 329.
[35] J. C. Conesa, Surf. Sci. 339 (1995) 337.
[36] R. Di Monte, J. Kašpar, J. Mater. Chem. 15 (2005) 633.
[37] S. Bedrane, PhD dissertation, Poitiers University, France, 2002.
[38] D. Martin, D. Duprez, J. Phys. Chem. 100 (1996) 9429.
[39] A. Holmgren, D. Duprez, B. Andersson, J. Catal. 182 (1999) 441.
[40] D. Duprez in "*Isotopes in Catalysis*" (J. Hargreaves et al. Eds), Chap. 7. Imperial College Press (2006).
[41] R. Kramer, M. Andre, J. Catal. 58 (1979) 287.
[42] D. Duprez, P. Pereira, A. Miloudi, R. Maurel, J. Catal., 75 (1982) 151.
[43] H. Kakioka, V. Ducarme and S. J. Teichner, J. Chim. Phys., 68 (1971) 1715.
[44] A. Galdikas, C. Descorme, D. Duprez, Solid State Ionics, 166 (2004) 147.
[45] A. Galdikas, C. Descorme, D. Duprez, Appl. Surf. Sci. 236 (2004) 342.
[46] A. Galdikas, C. Descorme, D. Duprez, F. Dong, H. Shinjoh, Topics Catal. 30/31 (2004) 405.
[47] D. Duprez, Stud. Surf. Sci. Catal. 112 (1997) 13.
[48] C. Li, K. Domen, K. Maruya, T. Onishi, J. Amer. Chem. Soc. 111 (1989) 7683.
[49] C. Li, K. Domen, K. Maruya, T. Onishi, J. Catal. 123 (1990) 436.
[50] J. G. Nunan, R. G. Silver, S. A. Bradley in "Catalytic Control of Air pollution" (R. G. Silver, J. E. Sawyer, J. C. Summers, Eds), ACS Symposium Series, Vol. 495 Chap. 7 (1992), p. 83.
[51] M. Ozawa, J. Alloys Comp. 275-277 (1998) 886.
[52] V. I. Parvulescu, P. Grange, B. Delmon, Catal. Today, 46 (1998) 233.
[53] Y. F. Yu Yao, Ind. Eng. Chem, Prod. Res. Dev. 19 (1980) 293.
[54] Y. F. Yu Yao, J. Catal. 87 (1984) 152.
[55] C. Serre, F. Garin, G. Belot, G. Maire, J. Catal. 141 (1993) 1.
[56] C. Serre, F. Garin, G. Belot, G. Maire, J. Catal. 141 (1993) 9.

[57] S. Johansson, L. Österlund, B. Kasemo, J. Catal. 201 (2001) 275.
[58] J. Barbier Jr, D. Duprez, Appl. Catal. B 3 (1993) 61.
[59] J. Barbier Jr, D. Duprez, in "*Steam effects in three-way catalysis*", a Review. Appl. Catal. B 4 (1994) 105.
[60] L. H. Dubois, P. K. Hansma, G. Somorjai, J. Catal. 65 (1980) 318.
[61] R. Dictor, J. Catal. 109 (1988) 89.
[62] F. Solymosi, L. Volgyesi, J. Rasko, Z. Phys. Chem. 120 (1980) 79.
[63] F. Solymosi, T. Bánsági, E. Novák, J. Catal. 112 (1988) 183.
[64] B. K. Cho, B. H. Shanks, J. E. Bailey, J. Catal. 115 (1989) 486.
[65] G. S. Zafiris, R. J. Gorte, J. Catal. 132 (1991) 275.
[66] J. Kaspăr, C. de Leitenburg, P. Fornasiero, A. Trovarelli, M. Graziani, J. Catal. 146 (1994) 136.
[67] T. P. Kobylinski, B. W. Taylor, J. Catal. 33 (1974) 376.
[68] K. Taylor, in "Catalysis, Science and Technology" (J. R. Anderson, M. Boudart, Eds), Vol. 5 p. 119. Springer Verlag, Berlin (1984).
[69] G. Leclercq, C. Dathy, G. Mabilon, L. Leclercq, in "Catalysis and Automotive Pollution Control CaPoC 2" (A. Crucq, Ed.). Stud. Surf. Sci. Catal. 71 (1991) 181.
[70] H. Muraki, G. Zhang, Catal. Today, 63 (2000) 337.
[71] J. L. Duplan, H. Praliaud, in "Catalysis and Automotive Pollution Control CaPoC 2" (A. Crucq, Ed.). Stud. Surf. Sci. Catal. 71 (1991) 667.
[72] N. K. Pande, A. T. Bell, J. Catal. 98 (1986) 7.
[73] W. C. Hecker, N. D. Wardinsky, P. G. Clemmer, P. B. Rasband, in "Progress in Catalysis". Proc. 12th Canadian Symp. Catal. (K. J. Smith and E. C. Sanford, Eds). Stud. Surf. Sci. Catal. 73 (1992) 211.
[74] S. H. Oh, J. Catal. 124 (1990) 477.
[75] S. H. Oh, C. C. Eickel, J. Catal. 128 (1991) 526.
[76] S. H. Oh, J. E. Carpenter, J. Catal. 101 (1986) 114.
[77] L. Pirault, P. Marecot, unpublished results.
[78] G. Djega-Mariadassou, F. Fajardie, J.-F. Tempère, J.-M. Manoli, O. Touret, G. Blanchard, J. Mol. Catal. 161 (2000) 179.
[79] G. Djega-Mariadassou, Catal. Today 90 (2004) 27.
[80] G. Ranga Rao, P. Fornasiero, R. Di Monte, J. Kaspar, G. Vlaic, G. Balducci, S. Meriani, G. Gubitosa, A. Cremona, M. Graziani, J. Catal. 162 (1996) 1.
[81] R. Di Monte, P. Fornasiero, M. Graziani, J. Kaspar, J. Alloys Comp. 275-277 (1998) 877.
[82] P. Fornasiero, G. Ranga Rao, J. Kaspar, F. L'Erario, M. Graziani, J. Catal. 175 (1998) 269.
[83] D. R. Mullins, S. H. Overbury, Surf. Sci. 511 (2002) L293.
[84] V. Schmatloch, I. Jirka, N. Kruse, J. Chem. Phys. 100 (1994) 8471.
[85] M. J. P. Hopstaken, J. W. Niemantsverdriet, J. Phys. Chem. 104 (2000) 3058.
[86] A. Martinez-Arias, J. Soria, J. C. Conesa, X. L. Seoane, A. Arcoya, R. Cataluña, J. Chem. Soc. Faraday Trans. 91 (1995), 1679..
[87] M. Haneda, Y. Kintaichi, H. Hamada, Phys. Chem. Chem. Phys, 4 (2002) 3146.

[88] J. J. Lecomte, P. Granger, L. Leclercq, J. F. Lamonier, A. Aboukais, G. Leclercq, Colloids and Surfaces A 158 (1999) 241.
[89] P. Granger, L. Delannoy, J. J. Lecomte, C. Dathy, H. Praliaud, L. Leclercq, G. Leclercq, J. Catal. 207 (2002) 202.
[90] F.B. Noronha, M.A.S. Baldanza, R.S. Monteiro, D.A.G. Aranda, A. Ordine, M. Schmal, Appl. Catal. A 210 (2001) 275.
[91] T. Kolli, K. Rahkamaa-Tolonen, U. Lassi, A. Savimäki, R. L. Keiski, Catal. Today 100 (2005) 297.
[92] J. R. Gonzalez-Velasco, M. A. Guttierez-Ortiz, J. L. Marc, M. Pilar Gonzalez-Marcos, G. Blanchard, Appl. Catal. B 33 (2001) 303.
[93] Z. Zu, C. Z. Wan, Y. K. Lui, J. Dettling, J. J. Steger, Catal. Today, 30 (1996) 83.
[94] A. Martínez-Arias, M. Fernández-García, A. Iglesias-Juez, A. B. Hungría, J. R. Anderson, J. C. Conesa, J. Soria, Appl. Catal. B 31 (2001) 51.
[95] T. Maunula, J. Ahola, T. Salmi, H. Haario, M. Härkönen, M. Luoma, V. J. Pohjola, Appl. Catal. B 12 (1997) 287.
[96] B. Harrison, M. Wyatt, K. C. Gough, in "Catalysis" (C. Kemball and D. A. Dowden, Eds). Vol. 5 p. 127. The Royal Society of Chemistry, London (1982).
[97] J. C. Vartui, R. D. Gonzalez, Ind. Eng. Chem., Proc. Res. Dev. 12 (1973) 265.
[98] J. W. Ault, R. J. Ayen, AIChE J. 17 (1971) 265.
[99] R. Pérez-Hernández, F. Aguilar, A. Gómez-Cortès, G. Díaz, Catal. Today, 107-108 (2005) 175.
[100] P. Bera, K. C. Patil, V. Jayaram, G. N. Subbanna, M. S. Hegde, J. Catal. 196 (2000) 293.
[101] R. Taha, D. Duprez, N. Mouaddib-Moral, C. Gauthier, in "Catalysis and Pollution Control CaPoC 4" (N Kruse, A. Frennet and J. M. Bastin, Eds), Stud. Surf. Sci. Catal. 116 (1998) 549.
[102] J. Fan, X. Wu, R. Ran, D. Weng, Appl. Surf. Sci. 245 (2005) 162.
[103] S. H. Overbury, D. R. Mullins, D. R. Huntley, L. Kundakovic, J. Catal. 186 (1999) 296.
[104] M. Daturi, N. Bion, J. Saussey, J. C. Lavalley, C. Hedouin, T. Seguelong, G. Blanchard, Phys. Chem. Chem. Phys. 3 (2001) 252.
[105] C. Thomas, O. Gorce, F. Villain, G. Djega-Mariadassou, J. Mol. Cat. A 249 (2006) 71.
[106] C. Thomas, O. Gorce, C. Fontaine, J. M. Krafft, F. Villain, G. Djega-Mariadassou, Appl. Catal. B 63 (2006) 201.
[107] T. Tanabe, M. Hatanaka, R. Tsuji, H. Shinjoh, R&D Review of Toyota CRDL, Vol. 37, Nr 3 (2002) 1.
[108] L F Cordoba, M. Flytzani-Stephanopoulos, C. Montes de Correa, Appl. Catal. B 33 (2001) 25.
[109] C. N. Costa, V. N. Stathopoulos, V. C. Belessi, A. M. Efstathiou, J. Catal. 197 (2001) 350.
[110] C. N. Costa, A. M. Efstathiou, J. Phys. Chem. B. 108 (2004) 2620.
[111] W. S. Epling, L. E. Campbell, A. Yezerets, N. W. Currier, J. E. Parks II, Catal. Rev. 46 (2004) 163.

[112] T. Nakatsuji, J. Ruotoistenmäki, V. Komppa, Y. Tanaka, T. Uekusa, Appl. Catal. B 38 (2002) 101.
[113] T. Kolli, U. Lassi, K. Rahkamaa-Tolonen, T-J. J. Kikunnen, R. L. Keiski, Appl. Catal. A 298 (2006) 65.
[114] L. F. Liotta, A. Macaluso, G. E. Arena, M. Livi, G. Centi, G. Deganello, Catal. Today 75 (2002) 439.
[115] M. Eberhardt, R. Riedel, U. Göbel, J. Theis, E. S. Lox, Topics Catal. 30/31 (2004) 135.
[116] S. Philipp, A. Drochner, J. Kunert, H. Vogel, J. Theis, E. S. Lox, Topics Catal. 30/31 (2004) 235.
[117] E.C. Corbos, S. Elbouazzaoui, X. Courtois, N. Bion, P. Marecot, D. Duprez, submitted in Topics in Catalysis (CaPoC 7).
[118] H.-Y. Lin, C.-J. Wu, Y.-W. Chen, C.-H. Lee, Ind. Eng. Chem. Res. 45 (2006) 134.
[119] M. Machida, D. Kurogi, T. Kijima, Catal. Today, 84 (2003) 201.